

Chitosan-magnesium aluminum silicate nanocomposite microspheres coated with poly(vinyl acetate phthalate) for controlled release of capecitabine

Sudha C. Angadi^{1*}, Lata S. Manjeshwar², Tejraj M. Aminabhavi³

¹Department of Chemistry, NMKRV College for Women, Bangalore 560 011, India

²Department of Chemistry, Karnataka University, Dharwad 58000, India

³Emeritus Fellow, All India Council for Technical Education, New Delhi, India.

SET's College of Pharmacy, Dharwad-580 002.

*Corresponding author

DOI: 10.5185/amp.2018/6659

www.vbripress.com/amp

Abstract

Nanocomposite microspheres of chitosan (CS) with magnesium aluminum silicate (MAS) and enteric coated with poly(vinyl acetate phthalate) (PVAP) have been prepared and examined for controlled release (CR) of capecitabine, an anticancer drug. The microspheres have been characterized by X-ray diffraction (XRD) to study the drug distribution, DSC to understand thermal stability and Fourier transform infrared (FTIR) spectroscopy to investigate the chemical interactions as well as to assess the structures of drug-loaded formulations. Surface morphology of the microspheres was investigated by scanning electron microscopy (SEM). The size distribution of the formulated microspheres studied by particle size analyzer was in the range of 303-350 μm , while their encapsulation efficiencies ranged from 50 to 58%. Equilibrium swelling of the microspheres was measured in both pH 1.2 and 7.4 media. *In vitro* release of capecitabine has shown a dependence on polymer-clay composition, amount of crosslinking agent and extent of enteric coating. The formulations extended the release of drug up to 32 h. The enteric coating with PVAP effectively reduced the burst release of the drug in gastric pH medium. The present method offers promising results for controlled release of short-acting drugs. Copyright © 2018 VBRI Press.

Keywords: Nanocomposites, chitosan, MAS, capecitabine, coating.

Introduction

Biopolymer-clay mineral nanocomposites are expected to impart novel properties compared to plain systems due to their plate-like structure that may affect their long term drug release characteristics. The advantages of nanocomposites such as good water absorption, swelling and cation exchange ability and those of chitosan (CS) were combined to introduce a carrier that could permit the intercalation of cationic CS in the expandable alumino-silicate structure of clay is expected to neutralize the strong binding of cationic drug by anionic clay; the solubility of CS at low pH of gastric fluid will decrease and premature release of the drug in the gastric environment can be minimized. Cationic chitosan provides the possibility of efficiently loading negatively charged drugs compared with clay; and the presence of reactive amine groups on CS provides ligand attachment sites for targeted delivery. The limited solubility of a CS-Clay nanocomposite drug carrier at gastric pH offers significant advantages for colon-specific delivery because some drugs are

destroyed in the stomach at acidic pH and in the presence of digestive enzymes. Furthermore, the muco-adhesive property of CS can enhance the bioavailability of drugs in the GI tract [1-7].

Capecitabine (CAP), a pro-drug, is widely used in the treatment of metastatic colorectal cancer as well as breast cancer and is readily absorbed from the gastrointestinal tract (GIT). It is converted to 5-fluorouracil in the body tissues following its oral administration. The recommended daily dose of the drug is high, i.e., 2.5 g/m² and it has a short elimination half-life of 0.5-1 h [8]. The adverse effects associated with CAP include bone-marrow depression, cardiotoxicity, diarrhea, nausea and vomiting, stomatitis, dermatitis, etc [9]. Hence, there is a need to develop the controlled release (CR) dosage forms of CAP to provide longer *in vitro* and *in vivo* antitumor activity, thereby reducing its immediate toxic side effects.

In this pursuit, it is of interest to select polymers that have appropriate chemical composition, physicochemical nature, biodegradability, chemical stability and excellent drug release characteristics [10].

In this work, we have chosen chitosan [poly (β -(1 \rightarrow 4)-2-amino-2-deoxy-d-glucose)], a deacetylated derivative of chitin, a naturally occurring polysaccharide found abundantly in marine crustaceans, insects and fungi [11]. The CS being a cationic biopolymer, it can interact with the negatively charged clay, which has a silicate layer structure. A very interesting possibility to modify drug release is to use clay-polymer nanocomposites. These nanocomposites offered the possibility of improving the properties of each single component and more frequently those of the polymer. Thus, the CS dispersions when mixed with clays, the hydrodynamic properties of the composite dispersions will alter [12-14]. In the literature, different types of clays such as montmorillonite [3, 15], magadiite [16] and rectorite [17] have been widely used to prepare biocompatible nanocomposite materials with CS.

Magnesium aluminum silicate (MAS) is a purified bentonite that has been widely used as a pharmaceutical excipient, e.g. as a suspending and stabilizing agent [18]; it is a mixture of colloidal montmorillonite and saponite that is composed of three-lattice layers with a central octahedral sheet of aluminum or magnesium and two external silica tetrahedron sheets [14]. The surface silicate layers of MAS have a negative charge, whereas edges of the layers have a positive charge. Electrostatic interactions between CS and MAS would therefore, cause a change in the flow behavior as well as zeta potential of the composite dispersions. Moreover, the interaction of CS with MAS would lead to flocculation in aqueous dispersions [13, 19].

The present study is aimed at developing novel type of nanocomposite microspheres of CS and MAS by the water/oil (w/o) emulsion crosslinking method using glutaraldehyde as a crosslinker. The microspheres were coated with a pH-sensitive enteric polymer viz., PVAP (polyvinyl acetate phthalate) to reduce the burst release of capecitabine. Recently, PVAP has been used for designing enteric coating formulations as tablets and capsules [20]. Therefore, in this work, we have selected PVAP for coating onto the drug-loaded microspheres of CS-MAS nanocomposites. The microspheres have been characterized by a variety of techniques to understand their size, morphology and chemical interactions between drug and polymer components. The *in vitro* release experiments of the developed formulations have been performed in pH 1.2 and 7.4 buffer media in order to understand the release patterns of the drug under the studied experimental parameters. Decreased toxicity potential, enhanced efficacy and targeted delivery will be the basis for continued usage of this nanocomposite in drug delivery system in the future.

Experimental

Preparation of nanocomposite microspheres

2% w/v. of CS (medium MW with 75-85% deacetylation, having a viscosity of 200-800 cps was purchased from Sigma-Aldrich, Mumbai, India) was

dispersed in 2% glacial acetic acid (s.d. fine chemicals Ltd. Mumbai, India) and the dispersion was stirred overnight at room temperature. 2% w/v. MAS (Himedia Laboratory Pvt. Ltd. Mumbai, India) was dispersed in hot water (deionised and double distilled) and then mixed with CS solution under stirring for 1 h. To this nanocomposite dispersion mixture, a required amount of CAP drug (Sun Pharmaceutical Ltd., Vadodara, India) was added and stirred for 1 h until complete dissolution. After the dissolution of drug, nanocomposite microspheres were prepared by using different ratios of CS and MAS by varying the amount of drug and crosslinking agent viz., glutaraldehyde (GA) (s. d. fine chemicals, Mumbai, India.) by the emulsion crosslinking method [21].

The above prepared nanocomposite dispersion was added slowly into 100g. w/w. light liquid paraffin oil (s. d. fine chemicals, Mumbai, India) containing 1% (w/w) Span 80 (Himedia Laboratory Pvt. Ltd. Mumbai, India) under a constant stirring speed of 400 rpm for about 15 min. To this w/o emulsion, the GA was added slowly under continuous stirring for 4 h. The hardened microspheres were then separated by filtration and washed repeatedly with *n*-hexane to remove the light liquid paraffin oil. The microspheres were further washed with 0.1 M glycine (Himedia Laboratory Pvt. Ltd. Mumbai, India) solution and water to remove the unreacted GA. Brady's test was performed to find any unreacted GA, but the test was negative, showing the absence of unreacted GA [22]. Solid microspheres obtained were vacuum-dried at 40°C for 24 h and stored in a desiccator until further use.

Coating of nanocomposite microspheres

The 1% (w/v) PVAP (s.d. fine Chemicals, Mumbai, India) dissolved in ethanol was used to coat the nanocomposite microspheres. To do this, nanocomposite microspheres were dissolved in 100 mL of 1% PVAP solution and stirred gently at 50 °C until all the solvent evaporated and formed a barrier layer of PVAP onto the surface of the nanocomposite microspheres. In all, seven formulations were prepared as per the formulation codes assigned in **Table 1**.

Table 1. Formulation parameters of the nanocomposite microspheres.

Formulation codes	CS (% w/w)	MAS (% w/w)	Drug (% w/w)	GA mL	PVAP (% w/w)
L1	100	-	5	5	1
L2	90	10	5	5	1
L3	80	20	5	5	1
L4	90	10	5	10	1
L5	90	10	10	5	1
L6	90	10	5	5	0
L7	90	10	-	5	1

Drug content

Estimation of drug concentration from the nanocomposite microspheres was done as per the method described by Rokhade *et al.*, [23]. Microspheres of known weight (10 mg) were ground to get the powder using an agate mortar, extracted with 50 mL of distilled water, stirred for 24 h and sonicated up to 60 min (UP 400s, Dr. Hielscher, GmbH, Germany). The solution was centrifuged (Jouan, MR23i, France) to remove polymeric debris and washed twice to extract the drug completely. The clear solution was analyzed by UV spectrophotometer (Secomam, Anthelie, France) at the λ_{\max} of 240 nm. The % drug loading and % encapsulation efficiency (EE) were calculated as:

$$\% \text{ Drug loading} = \left(\frac{\text{Weight of drug in microspheres}}{\text{Weight of microspheres}} \right) \times 100 \quad (1)$$

$$\% \text{ Encapsulation efficiency} = \left(\frac{\text{Actual drug loading}}{\text{Theoretical drug loading}} \right) \times 100 \quad (2)$$

Equilibrium swelling experiments

Equilibrium swelling of nanocomposite microspheres was determined gravimetrically by measuring the extent of swelling in pH 1.2 as well as pH 7.4 media. To ensure complete equilibration, samples were allowed to swell for 24 h and the excess surface-adhered liquid droplets were removed by blotting with a soft tissue paper. The swollen microspheres were weighed to an accuracy of ± 0.01 mg on an electronic microbalance (Mettler, model AT120, Greifensee, Switzerland). The nanocomposite microspheres were dried in an oven at 60 °C for 5 h until no weight gain of the dried samples was observed to calculate the % equilibrium swelling [24]:

$$\% \text{ Swelling} = \left[\frac{W_s - W_d}{W_d} \right] \times 100 \quad (3)$$

where W_s is weight of the swollen microspheres and W_d is weight of the dry microspheres. Experiments were performed in triplicate, but the average values reproduced within $\pm 3\%$ standard errors were considered in data analysis and graphical display. The % swelling results are included in **Table 2**.

Table 2. Results of % encapsulation efficiency (EE), particle size, % swelling, n and k parameters of eqn. (4) along with correlation coefficients (r^2).

Formulation codes	EE (%)	Size (μm)	Swelling (%)		n	k	r^2
			pH 1.2	pH 7.4			
L1	50	200	450	600	0.43	0.226	0.964
L2	52	303	400	521	0.51	0.175	0.983
L3	55	310	340	467	0.52	0.184	0.96
L4	58	210	299	405	0.61	0.123	0.977
L5	51	300	375	472	0.51	0.18	0.975
L6	50	350	550	530	0.48	0.236	0.913

In vitro drug release experiments

Drug release from the coated nanocomposite microspheres containing different CS and MAS compositions, extent of crosslinking and enteric coating were investigated in pH 1.2 for the initial 2 h, followed by the release in phosphate buffer of pH 7.4 until the completion of the dissolution process. These experiments were performed in triplicate in a tablet dissolution tester (LabIndia, Disotest, Mumbai, India) equipped with eight baskets (glass jars) at the stirring speed of 100 rpm. Weighed quantity of each sample was placed in 500 mL of dissolution media maintained at 37 °C. At regular intervals of time, sample aliquots were withdrawn and analyzed using UV spectrophotometer (Secomam, Anthelie, France) at the fixed λ_{\max} of 240 nm.

Characterization

Fourier Transform Infrared (FTIR) spectral measurements

FTIR spectra were obtained using Nicolet (Model Impact 410, Milwaukee, WI, USA) instrument to confirm the formation of nanocomposite structure as well as to confirm any chemical interactions of CAP with the polymer. FTIR spectra of CS, MAS, nanocomposite microspheres of CS-MAS, placebo nanocomposite microspheres, pristine capcitabine drug and drug-loaded nanocomposite microspheres were all taken by grinding separately with KBr powder and making pellets under a hydraulic pressure of 600 kg/cm². Spectral scanning was done in the range of 4000 to 500 cm⁻¹.

Differential Scanning Calorimetry (DSC)

Differential scanning calorimetry (DSC-Q20, TA Instruments-Waters, USA) was performed on placebo nanocomposite microspheres, pristine CAP and CAP-loaded nanocomposite microspheres by heating the samples from 25°C to 400°C at the heating rate of 10°C/min in a nitrogen atmosphere.

X-ray diffraction (XRD)

Intercalation of chitosan into MAS structure as well as crystallinity of CAP after encapsulation were evaluated

by XRD recorded on the nanocomposite microspheres with CAP and without CAP as well as pristine CAP and MAS using X-ray diffractometer (x-Pert, Philips, UK). Scanning was done up to 2θ of 80° .

Scanning electron microscopy (SEM)

SEM images were taken using a JEOL model JSM-840A, Japan instrument (STIC, Cochin University, Kochi, India). Nanocomposite microspheres were sputtered with gold to make them conducting and placed on a copper stub. Thickness of the gold layer accomplished by gold sputtering was about 10 nm.

Particle size measurements

Particle size and size distributions were measured using a mastersizer (Malvern, model MS-2000, UK). Particle size data are included in **Table 2**.

Results and discussion

Fourier transform infrared spectral study

FTIR spectra of (**Fig. 1a**) CS, MAS and placebo microspheres (L7) were taken to prove the nanocomposite structure. FTIR spectrum of CS (**Fig. 1a(A)**) showed a broad band at 3450 cm^{-1} , which is attributed to O-H stretching vibrations, while the bands at 2922 cm^{-1} and 2810 cm^{-1} represent the presence of C-H aliphatic stretching vibrations. Three bands appearing at 1660 cm^{-1} , 1590 cm^{-1} and 1379 cm^{-1} are assigned to amide-I, amide-II and amide-III, respectively. The CS is characterized by its saccharide structure at 899 cm^{-1} and 1154 cm^{-1} . FTIR spectrum of MAS (**Fig. 1a(B)**) showed hydroxyl stretching of SiOH at 3590 cm^{-1} , hydroxyl stretching of H_2O at 3400 cm^{-1} , hydroxyl bending of H_2O at 1630 cm^{-1} and stretching of Si-O-Si at 1010 cm^{-1} [25]. The effects of hydrogen-bonding were taken into account for the intercalation of chitosan chain into negatively charged clay [26]. The amide bands for placebo microspheres (90 wt.% chitosan with 10 wt.% clay without drug) are shifted towards lower wave number values as shown in **Fig. 1a(C)**, indicating a possible formation of hydrogen-bonding between the clay and CS. Meanwhile, OH group appearing at 3450 cm^{-1} in the case of CS is shifted towards lower wave number in placebo microspheres, suggesting enhanced hydrogen-bonding interaction between the CS and the MAS [27], hence the formation of nanocomposite structure is proved.

Fig. 1b, shows the FTIR spectra of CAP drug, placebo microspheres and drug-loaded microspheres. Pristine CAP showed characteristic bands due to different functional groups, but the bands appearing at 3530 cm^{-1} and 3260 cm^{-1} are due to O-H/N-H stretching vibrations. The band at 1700 cm^{-1} is due to pyrimidine carbonyl stretching vibrations, whereas the bands at 1720 cm^{-1} and 1760 cm^{-1} are due to urethane carbonyl stretching vibrations. Characteristic bands at 1050 cm^{-1} and 1200 cm^{-1} indicate C-F stretching vibrations as well as the presence of tetrahydrofuran ring, respectively. After incorporating capecitabine into

the nanocomposite matrix, in addition to characteristic bands of placebo microspheres (L7), some additional bands have appeared due to the presence of capecitabine. Notice that the characteristic bands of capecitabine observed at 1050 cm^{-1} , 1200 cm^{-1} and 1720 cm^{-1} have also appeared in the drug-loaded matrix without any change, indicating the chemical stability of CAP in the formulation [27].

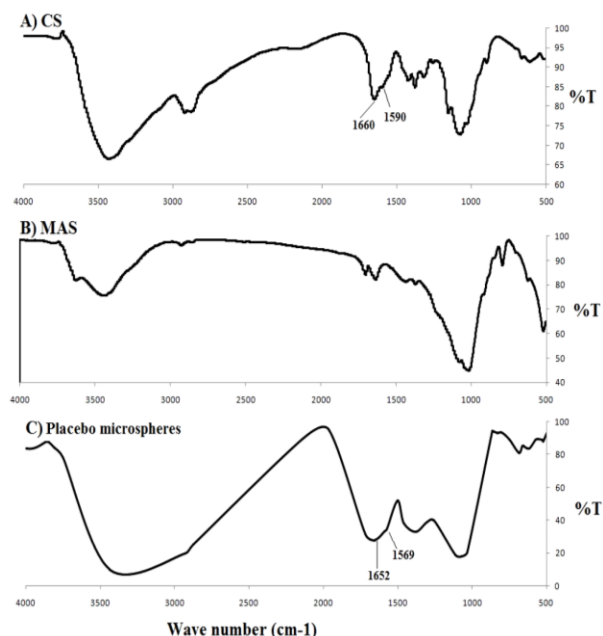


Fig. 1a. FTIR spectra of (A) CS, (B) MAS and (C) placebo microspheres.

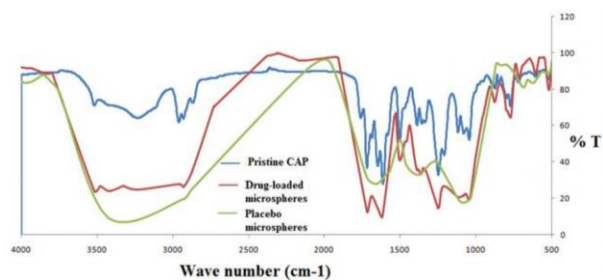


Fig. 1b. FTIR of pristine CAP, placebo microspheres and drug-loaded microspheres.

Differential Scanning Calorimetry (DSC)

DSC was used to study thermal transitions during the heating cycles under an inert atmosphere. DSC thermograms of placebo nanocomposite microspheres, pristine CAP and CAP-loaded nanocomposite microspheres are displayed in **Fig. 2**. In the case of pristine CAP, two endothermic peaks are observed, one at 122°C , corresponding to melting process and the other at 150°C due to thermal decomposition [27]. Thermograms of placebo nanocomposite microspheres showed endothermic peaks at 104°C , 200°C and 340°C . Similarly, drug-loaded microspheres have shown the same pattern as that of placebo, but no peaks are

observed at 122°C and 150°C, indicating the amorphous dispersion of capecitabine in the composite matrix.

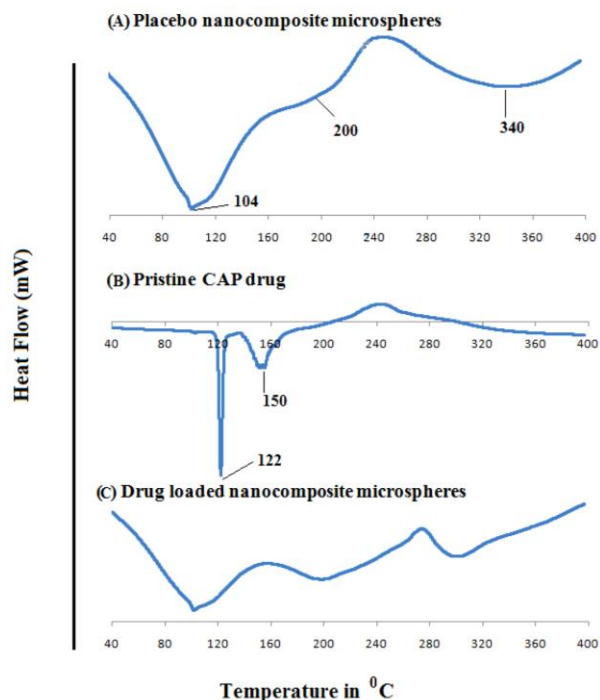


Fig. 2. DSC of (A) placebo nanocomposite microspheres, (B) pristine CAP drug and (C) drug- loaded nanocomposite microspheres.

X-ray diffractometry (XRD)

The X-ray diffraction spectra recorded for (A) placebo nanocomposite microspheres (B), pristine CAP (C) CAP-loaded nanocomposite microspheres and (D) MAS are presented in **Fig. 3**. The MAS has characteristic peaks at 2θ of 8.5° and 28.1°. The peak at 8.5° is shifted to lower 2θ value of 5° and a peak at 28.1° is shifted to 27° in the placebo nanocomposite microsphere as well as in drug loaded microspheres indicating the inter layer spacing of MAS and hence intercalation of chitosan in to MAS structure. CAP has characteristic intense peaks at 2θ of 5°, 20° and 25°, but in case of both CAP-loaded and placebo matrices, no intense peaks are observed at 2θ of 5°, 20° and 25°. Also, diffractograms of both CAP-loaded and placebo composite microspheres are almost identical, indicating the amorphous dispersion of CAP after encapsulation into the composite matrix [27].

Scanning Electron Microscopy (SEM)

SEM images of group of particles and single particle taken at different magnifications indicate clustered shapes (**Fig. 4A-D**). Coated microspheres have rough and wrinkled surfaces without pores, whereas uncoated microspheres have pores on their surfaces. The surface of a single microsphere of uncoated L2 formulation appears to be porous, whereas the surface of coated L2 formulation has wrinkled rough surface, but without the presence of pores.

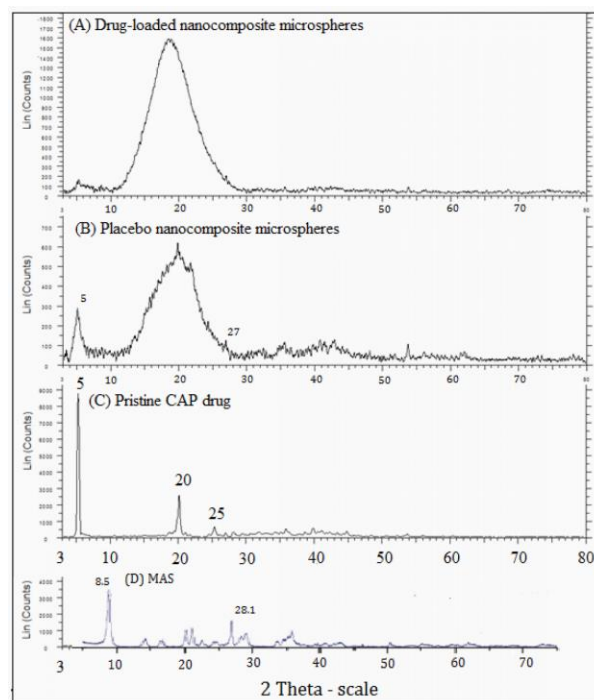


Fig. 3. XRD of (A) drug-loaded nanocomposite microspheres, (B) placebo nanocomposite microspheres (C) pristine CAP drug and (D) MAS.

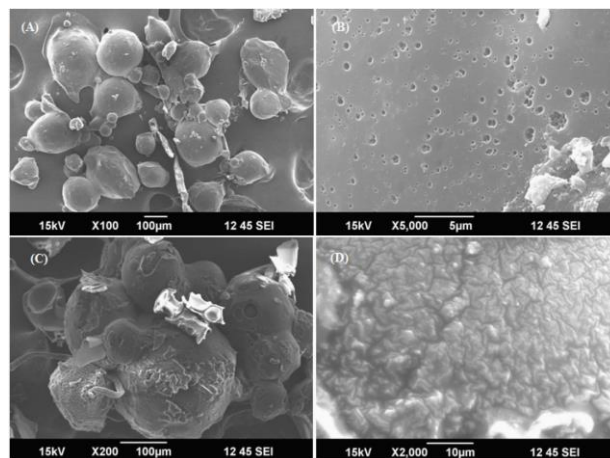


Fig. 4. SEM pictures of (A) group of microspheres of uncoated L6 formulation, (B) surface of single microsphere of uncoated L6 formulation, (C) group of microspheres of coated L2 microspheres and (D) surface of single microsphere of coated L2 formulation.

Particle size

The results of mean particle size are presented in **Table 2**, while the size distribution curve for typical formulations, viz., uncoated L2 and coated L2 formulations containing 90 wt. % CS, 10 wt. % MAS with 5 wt. % CAP and 5 mL of GA are displayed in **Figs. 5A and B**, respectively. Size of the microspheres depends on polymer-clay composition, enteric coating and extent of cross-linking agent used. Particle size range between 200 μm and 350 μm , but with increasing concentration of MAS, the size has increased from 303

μm to $310 \mu\text{m}$. The particle size of L3 (20% w/w, MAS) is higher than that of L2 (10% w/w, MAS) formulation, suggesting higher the concentration of MAS, higher will be the viscosity of the dispersion [13], thereby increasing the droplet size during the formation of the microspheres. Size of the coated microspheres is always less than those of the uncoated microspheres, probably due to the compression of the polymer matrix, since electrostatic interaction exists between CS and the coated PVAP. The particle size decreases with increasing crosslinking as observed with L4, and its size is less than L2 due to the compression of network structure at higher crosslinking.

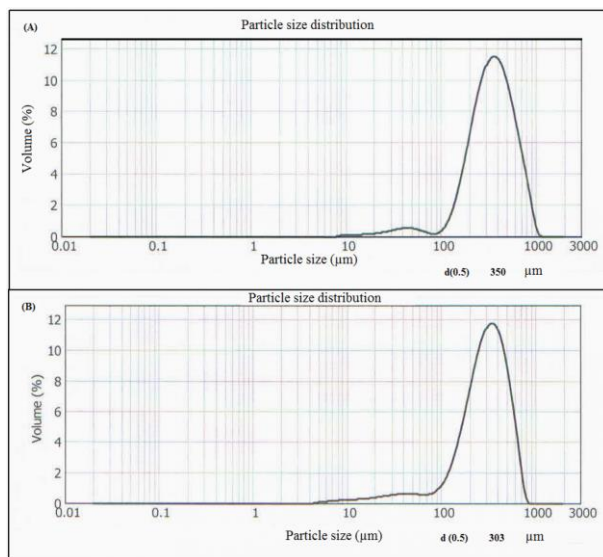


Fig. 5. Particle size distribution curves of (A) L6 and (B) L2 formulations.

Encapsulation Efficiency (EE)

In order to achieve high % EE, formulation process variables such as polymer-clay ratio and extent of crosslinking are important. Thus, by increasing the amount of MAS, a slight increase in % EE is observed due to increase in the viscosity of polymer-clay dispersion, thereby trapping more of CAP particles. With increasing concentration of crosslinking agent, EE also increases, since the rigid network retains more of drug particles.

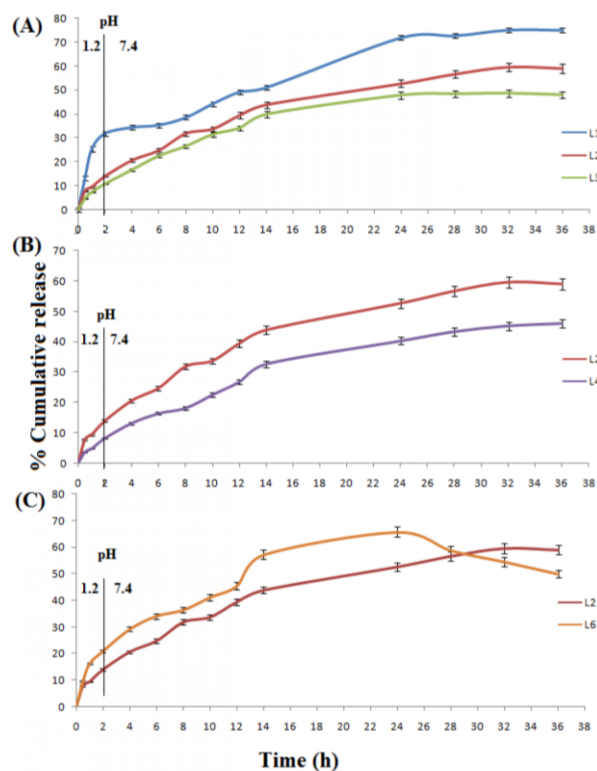
Equilibrium swelling study

Drug release from the polymer-clay nanocomposite microspheres is greatly influenced by the equilibrium swelling of the matrix in buffer media of pH 1.2 and 7.4. Coated microspheres swell to a lesser extent in pH 1.2 than the uncoated microspheres, due to the intact PVAP coating onto the surface of the microspheres, but the uncoated microspheres are more swollen in pH 1.2 media because the CS carries a net positive charge in acidic pH and hence, their chains repel each other, resulting in a higher swelling. In phosphate buffer solution (pH 7.4), coated microspheres are more

swollen than the uncoated microspheres, since in the alkaline media, coated PVAP ionizes, thereby allowing the penetration of more drug solution into the nanocomposite microspheres compared to the uncoated microspheres.

The % equilibrium swelling data of the crosslinked microspheres presented in **Table 2** indicate that as the amount of GA in the matrix is increased from 5 to 10 mL, equilibrium swelling decreased significantly due to a reduction in swelling capacity of the rigid matrix at higher crosslink density. Notice that formulations containing higher amount of MAS exhibit lower swelling due to the rigid nature of the matrix. For instance, formulation L2 (10 wt. % of MAS) exhibits lower swelling than L1 (0 wt. % MAS), thereby restricting the nanocomposite to absorb lesser amount of aqueous media.

Fig. 6. (A) Effect of polymer-clay composition, (B) effect of crosslinking agent and (C) effect of enteric coating on *in-vitro* release of CAP from nanocomposite microspheres.



In-vitro release

In vitro release data are discussed in terms of the effect of polymer-clay composition, amount of crosslinking agent and the extent of enteric coating with PVAP. The *in vitro* release experiments were conducted in pH 1.2 for the initial 2 h followed by phosphate buffer of pH 7.4 until the completion of dissolution process. The average % cumulative release vs. time plots of the triplicate data for all the formulations are displayed in **Figs. 6a, 6b and 6c**. Error bars indicate the maximum of $\pm 3\%$ standard deviations from the average values used to construct the smoothed release curves.

Effect of polymer-clay composition

As displayed in **Fig. 6a**, the L3 has a lesser release rate than L2, and L2 has a lesser release rate than L1. Since L3 has a higher content of MAS (20% w/w.), higher will be the viscosity of the polymer-clay mixture solution and intercalation of chitosan chains into silicate layers of MAS i.e., greater electrostatic interaction between the positively charged protonated amino groups of CS and the negatively charged surfaces of silicate layers of MAS as per the intercalation model displayed in **Fig. 7**. Hence, the matrix is denser than L2 or L1 that contained 10% and 0% w/w. of MAS, respectively. In all the formulations, the *in vitro* release profiles follow identical patterns and the release of CAP is extended up to 32 h, suggesting its utility in oral dosage formulations of CAP. Also, % release of CAP is higher in pH 7.4 than in pH 1.2 media for all the coated formulations.

Effect of crosslinking

As displayed in **Fig. 6b**, formulation L4 has a lower release rate than L2 as L4 containing 10 mL of GA is highly crosslinked and hence, is a stronger network matrix compared to L2, which contains 5 mL of GA. The L4 released nearly 46 % of CAP in about 36 h, whereas L2 released 60% in 32 h.

Effect of enteric coating

The 1% w/w. PVAP coating was used to coat the microspheres in all the formulations. **Fig. 6c** shows higher CAP release in case of L6 compared to L2. About 59 % CAP was released in 32 h from the coated L2 formulation, whereas nearly 66% of CAP was released from the uncoated L6 formulation in 24 h. The burst release in gastric media (pH 1.2) from the uncoated L6 formulation was reduced by coating onto the surface of the nanocomposite microspheres, which also controlled the drug release in pH 7.4 media.

Empirical correlation

To understand the molecular transport of CAP through the studied polymer-clay nanocomposite microspheres, the cumulative release data have been fitted to the empirical equation [28]:

$$M_t / M_\infty = kt^n \quad (4)$$

where M_t/M_∞ represents the fractional release of CAP at time, t ; k is a characteristic interaction parameter of CAP-polymer composite system and n is an empirical parameter characterizing the release mechanism. Using the least-squares procedure at 95% confidence limit, we have estimated the values of n and k for all the six formulations both in pH 1.2 and 7.4 media and these data along with the estimated correlation coefficients are included in **Table 2**. For the values of $n = 0.5$, drug diffuses and releases out of the polymer matrix following the Fickian diffusion. For $n > 0.5$, anomalous or non-Fickian transport operates. If $n = 1$, non-Fickian or more commonly called Case II transport occurs.

If $n > 1$, the non-Fickian Super Case II is operative. If the values of n vary between 0.5 and 1.0, then transport is classified as anomalous type [29].

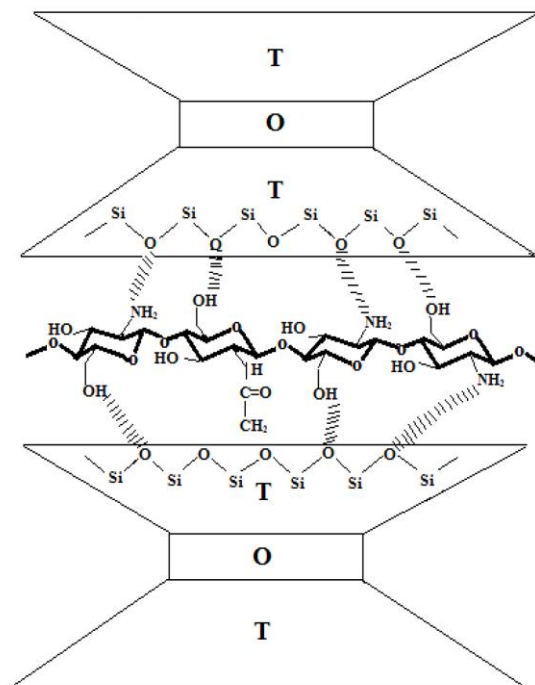


Fig. 7. Schematic representation of the intercalation of chitosan chains into silicate layers of MAS forming the nanocomposite.

where T – tetrahedral sheet of MAS plate
O – octahedral sheet of MAS plate

In this study, the values of n and k are dependent on polymer-clay composition, concentration of crosslinking agent and enteric coating. The values of k decrease with increasing concentration of MAS. The n value for coated L2 formulation is higher than the uncoated formulation L6, due to the formation of intact outer barrier layer of PVAP, thereby reducing the burst release of CAP in acidic medium, thus facilitating the CR of CAP in pH 7.4 media. The values of n are higher for the nanocomposite microspheres due to the formation of a strong network matrix to hold the drug particles and are higher for those that contain higher amount of MAS. In the present work, the n values for all the coated nanocomposite microspheres range from 0.513 to 0.606, indicating that CAP release from the microspheres follows the anomalous type transport.

Conclusion

This study demonstrates the development of a novel nanocomposite polymer-clay microsphere device consisting of chitosan-MAS enteric coated with poly(vinyl acetate phthalate) prepared by emulsion crosslinking method using glutaraldehyde as a crosslinker to achieve the CR of capecitabine. The prepared microspheres have the sizes ranging from

210 μm to 350 μm . The formulations released capecitabine in a controllable manner extending its plasma half life of 0.5-1 h to 32 h with a cumulative release of 60% CAP. The enteric coating with PVAP was effective in retarding the release of CAP in the gastric stomach media that helped for the controlled release of CAP in the intestinal pH 7.4 media. The release of water-soluble CAP, as analyzed by an empirical equation, suggested the anomalous nature. The present method may be applicable for the preparation of other micro-devices for the CR of short-acting drugs.

Acknowledgments

The authors (Dr. Sudha C. Angadi thank the University Grants Commission (UGC), New Delhi, India (1378-MRP/14-15/KABA035/UGC-SWRO) for a MRP fellowship to Dr. S. C. Angadi. Professor T.M. Aminabhavi thanks the All India Council for Technical Education [F. No. 1-51/RIFD/EF4 (13)], New Delhi, India for an Emeritus Fellowship.

References

1. John, J. J. Thomas, S. (Eds.) Natural Polymers, RSC Green Chemistry Series, **2012**, 2, 59.
2. Eugene Khor, Andrew C. A.; (Eds.) Chitin; Fulfilling a Biomaterials Promise, Elsevier Ltd. **2014**.
3. Wang, S. F.; Shen, L.; Tong, Y.J.; Chen, L.; Phang, I. Y.; Lim, P.Q. *Polym. Degrad. Stab.* **2005**, 90, 123.
DOI: 10.1016/j.polymdegradstab.2005.03.001
4. Depan, D.; Kumar, A. P.; Singh, R. P.; *Acta Biomater.* **2009**, 5, 93.
DOI: 10.1016/j.actbio.2008.08.007.
5. Aguzzi, C.; Cerezo, P.; Viseras, C.; Caramella, C.; *Appl. Clay Sci.* **2007**, 36, 22.
DOI: 10.1016/j.clay.2006.06.015
6. Byrne, R. S.; Deasy, P. B.; *J. Microencapsul.* **2005**, 22, 423.
DOI: 10.1080/02652040500100196
7. Lin, J. J.; Wei, J. C.; Juang, T. Y.; Tsai, W. C.; *Langmuir.* **2007**, 23, 1995.
DOI: 10.1021/la062013h
8. Judson, I. R.; Beale, P. J.; Trigo, J. M.; Aherne, W.; Crompton, T.; Jones, D.; Bush, E.; Reigner, B.; *Invest. New Drugs.* **1999**, 17, 49.
DOI: 10.1023/A: 1006263400888
9. Agnihotri, S. A.; Aminabhavi, T. M.; *Int. J. Pharm.* **2006**, 324, 103.
DOI: 10.1016/j.ijpharm.2006.05.061
10. Doelker, E.; CRC Press, Boca Raton, FL, **1987**, 115.
11. Agnihotri, S. A.; Mallikarjuna, N. N.; Aminabhavi, T. M.; *J. Controlled Release.* **2004**, 100, 5.
12. Günster, E.; Pestreli, D.; Ünlü, C. H.; Atıcı, O.; Güngör, N.; *Carbohyd. Polym.* **2007**, 67, 358.
DOI: 10.1016/j.carbpol.2006.06.004
13. Khunawattanukul, W.; Puttipipatkachorn, S.; Rades, T.; Pongjanyakul, T.; *Int. J. Pharm.* **2008**, 351, 227.
DOI:10.1016/j.ijpharm.2007.09.038
14. Alexandre, M.; Dubois, P.; *Mater. Sci. Eng.* **2000**, 28, 1.
DOI: 10.1016/S0927-796X(00)00012-7
15. Darder, M.; Colilla, M.; Ruiz-Hitzky, E.; *Appl. Clay Sci.* **2005**, 28, 199.
DOI: 10.1016/j.clay.2004.02.009
16. Liu, K. H.; Liu, T. Y.; Chen, S.Y.; Liu, D.M.; *Acta Biomater.* **2007**, 3, 919.
DOI: 10.1016/j.actbio.2007.06.002
17. Wang, X.; Du, Y.; Luo, J.; Lin, B.; Kennedy, J. F.; *Carbohyd. Polym.* **2007**, 69, 41.
DOI: 10.1016/j.carbpol.2006.08.025
18. Kibbe, H. A.; (3rd ed); Handbook of Pharmaceutical Excipients; American Pharmaceutical Association: Washington, **2000**.
19. Khunawattanukul, W.; Puttipipatkachorn, S.; Rades, T.; Pongjanyakul, T.; *Int. J. Pharm.* **2010**, 393, 220.
DOI:10.1016/j.ijpharm.2010.04.007
20. Abdel, N. Z.; Qaddomi, A.; *Pak. J. Pharm. Sci.* **2012**, 25, 59.
ICID: 971303
21. Rokhade, A. P.; Agnihotri, S. A.; Patil, S. A.; Mallikarjuna, N. N.; Kulkarni, P. V.; *Carbohyd. Polym.* **2006**, 65, 243.
DOI:10.1016/j.carbpol.2006.01.013
22. Agnihotri, S. A.; Aminabhavi, T. M.; *J. Controlled Release.* **2004**, 96, 245.
DOI:10.1016/j.jconrel.2004.01.025
23. Rokhade, A. P.; Shelke, N. B.; Patil, S. A.; Aminabhavi, T. M.; *Carbohyd. Polym.* **2007**, 69, 678.
DOI:10.1016/j.carbpol.2007.02.008
24. Haragopad, S. B.; Aminabhavi, T. M.; *Macromol.* **1991**, 24, 2598.
DOI: 10.1021/ma00009a070
25. Angadi, S. C.; Manjeshwar, L. S.; Aminabhavi, T. M.; *Int. J. Bio. Macromol.* **2012**, 51, 45.
DOI:10.1016/j.ijbiomac.2012.04.018
26. Chen, P.; Zhang, L. N.; *Biomacromol.* **2006**, 7, 1700.
DOI: 10.1021/bm050924k
27. Tanga, C.; Chena, N.; Zhanga, Q.; Wanga, K.; Fua, Q.; Zhang, X.; *Polym. Degrad. Stab.* **2009**, 94, 124.
DOI:10.1016/j.polymdegradstab.2008.09.008
28. Ritger, P. L.; Peppas, N. A.; *J. Controlled Release* **1987**, 5, 37.
DOI: 10.1016/0168-3659(87)90035-6
29. Mundargi, R. C.; Shelke, N. B.; Rokhade, A. P.; Patil, S. A.; Aminabhavi, T. M.; *Carbohyd. Polym.* **2008**, 71, 42.
DOI: 10.1016/j.carbpol.2007.05.013